

Relaxation mode coupling and universality in stress–strain cycles of networks including the glass transition region

V. Kraus*, H.-G. Kilian and M. Saile

Abteilung Experimentelle Physik, Universität Ulm, D-89069 Ulm, Germany

(Received 22 January 1993; revised 22 October 1993)

The temperature and strain rate dependence of stress–strain cycles of poly(methyl methacrylate) (PMMA) networks are investigated. The van der Waals theory of polymer networks describes the quasi-static stress–strain behaviour. Time-dependent effects during deformation are treated within the framework of irreversible thermodynamics. The Gibbs function of the network is extended by an appropriate set of hidden variables. The orthogonal relaxation modes of the Onsager type, represented by these hidden variables, couple in an isotropic and scalar manner with the network (relaxation mode coupling model). The time dependence of the nominal force is characterized by a relaxation time distribution that is independent of strain and of the deformation mode. In the thermodynamic limit the strain-energy of the network is the fundamental state of reference even at large strains. In the rubbery region the Williams–Landel–Ferry (WLF) equation describes thermorheological simple behaviour. In the glass transition region, the WLF-shift procedure fails when the mean relaxation time becomes large (WLF boundary). A specific, but universal modification of the WLF-shift procedure due to the strain-induced process of polymer segments changing place is observed and results in a unique frequency–temperature relationship (elastic and rheological simple behaviour).

(Keywords: stress–strain curves; polymer networks; relaxation glass transition)

INTRODUCTION

To improve our understanding of the vitrification of amorphous polymers, we present research about large deformations of permanent networks carried out in the rubbery state and in the glass transition region. Stress–strain cycles, performed at various temperatures and different strain rates, reveal universal features of solidification.

The time-dependent phenomena of rubbers observed in stress–strain cycles at different temperatures and under different strain rates^{1,2} are well understood within the framework of the thermodynamics of irreversible processes^{3–6}. The Gibbs function of a van der Waals network, as used for the description of equilibrium stress–strain curves, is extended by an adequate set of hidden variables^{7–9} to describe non-equilibrium states as well. The relaxation time spectrum¹⁰, defined by these hidden variables, characterizes elementary relaxation processes. These processes are coupled with the network in a linear and scalar form (relaxation mode coupling model). The treatment leads to the consequence that the relaxation time spectrum is strain invariant. The relaxation time spectrum, measured at small distortions under shear¹¹, defines the memory function which is independent of strain and of the deformation mode. This memory function typifies each individual network. The network itself shows thermorheological simple behaviour. This particular situation allows us to calculate stress–strain

cycles of networks at each temperature at different strain rates up to large strains^{12,13}.

Within the glass transition region, stress–strain cycles become increasingly non-linear the lower the initial sample temperature. It is of interest to reveal the reason for this phenomenon. The Williams–Landel–Ferry (WLF) method^{14,15} proposes that the relaxation mechanisms should always behave in a similar fashion¹⁶. To defend this hypothesis, we should keep in mind that the master curve construction includes relaxation processes for the shortest periods of time in the glassy state and for the longest periods of time in the rubbery state. The glass transition region includes all the processes in between. Therefore, there is no logical reason to expect new relaxation mechanisms during deformation in the glass transition region. Under these circumstances, it appears to be justified to apply the relaxation mode coupling model in this temperature range. This paper represents a first step in developing a phenomenological description of the strain-rate dependent deformation of networks in the rubbery state and in the glass transition region. We do not try to explain the formation of a neck^{17,18}.

THE EQUILIBRIUM STRESS–STRAIN CURVE OF RUBBER

In order to describe non-equilibrium states or deviations from equilibrium, we have to define the corresponding equilibrium state first. Our aim is to look at the relaxation behaviour of highly stretched networks, so we need a description of equilibrium stress–strain curves that yields

* To whom correspondence should be addressed

good accordance with experiments over the whole range of applied strain. For this reason, we use the model of the van der Waals network. From the strain energy function W of the van der Waals network²:

$$W(\lambda) = -G \left\{ 2\phi_m [\ln(1-\eta) + \eta] + \frac{2}{3} a\phi(\lambda)^{3/2} \right\} = Gw(\lambda) \quad (1)$$

the nominal force f is obtained by differentiating W with respect to the macroscopic strain $\lambda = L/L_0$ (where L_0 is the initial length of the sample, and L is the length during deformation):

$$f(\lambda) = \frac{\partial W(\lambda)}{\partial \lambda} = GD(\lambda) \left[\frac{1}{1-\eta} - a\phi^{1/2}(\lambda) \right] \quad (2)$$

In the mode of simple extension $\phi(\lambda)$ is given by:

$$\phi(\lambda) = \frac{1}{2} \left(\lambda^2 + \frac{2}{\lambda} - 3 \right) \quad (3)$$

Equations (1) and (2) use the terms $\phi_m = \phi(\lambda_m)$, $\eta = \sqrt{\phi(\lambda)/\phi_m}$ and the deformation function:

$$D(\lambda) = \partial_\lambda \phi(\lambda) \quad (4)$$

The first of the strain independent van der Waals parameters, the maximum strain λ_m , defines the maximum chain extensibility in networks with finite chain length. It interrelates the molecular weight M_c of the polymer chain between two crosslinks with M_u :

$$M_c = M_u \lambda_m^2 \quad (5)$$

where M_u is the molecular weight of the stretching invariant unit of the polymer chain. The second van der Waals parameter a characterizes global interactions between the network chains^{1,18}. The shear modulus G of a permanent network¹⁹ is given by:

$$G = \frac{\rho RT}{M_u \lambda_m^2} \quad (6)$$

where R is the gas constant, T is the absolute temperature and ρ is the density of the polymer. As seen from Figure 1, the equilibrium stress-strain curve computed with equation (2) reproduces the experimental data very accurately. Hence, if the fundamental network parameters M_u , λ_m and a are known, the equilibrium state of reference is well defined.

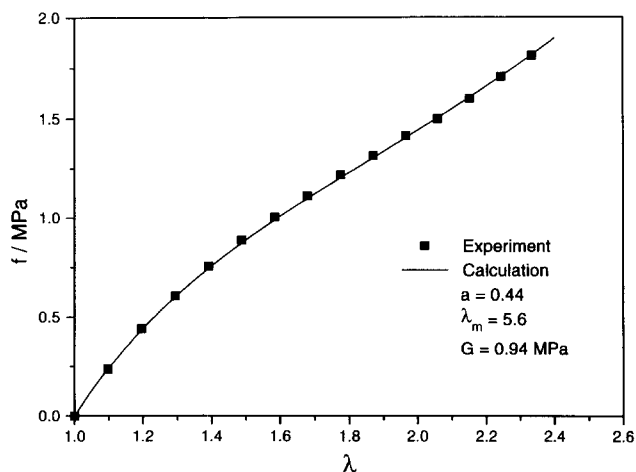


Figure 1 Equilibrium stress-strain curve of crosslinked PMMA at 413 K

A NON-EQUILIBRIUM DESCRIPTION OF STRAINED NETWORKS

In equilibrium thermodynamics, a system is fully determined by a Gibbs function in its natural variables²⁰. The differential of the Gibbs free energy density of a permanent network at constant pressure is written as:

$$dg = -s dT + f d\lambda \quad (7)$$

where s is the entropy density. The last term is the energy form which describes the work exchanged under constant volume conditions. For networks, equation (7) was shown to be correct up to large strains².

Using the assumption that networks cannot be forced into states which are far from equilibrium, linear material equations are applicable. We are then allowed to use the thermodynamics of irreversible processes. The differential of the Gibbs free energy density⁷ is extended by introducing a set of time- and temperature-dependent hidden variables ξ_i (ref. 3):

$$dg = -s dT + f d\lambda - \sum_i A_i d\xi_i \quad (8)$$

Relaxation processes are described by the time dependence of these hidden variables. Considering polymer networks, it is crucial that the relaxation mechanisms should be coupled with the strain energy of the network. An adequate formulation of this relaxation mode coupling starts by defining a Gibbs free energy density for isothermal and isobaric conditions by the homogeneous quadratic form²:

$$g = \frac{1}{2} f_{20} w(\lambda) + \sqrt{w(\lambda)} \sum_i f_{11}^{(i)} \xi_i + \frac{1}{2} \sum_i f_{02}^{(i)} \xi_i^2 \quad (9)$$

where the second term on the right-hand side represents the coupling of the relaxation modes to the network. The relaxation of the i th process shall now satisfy the linear Onsager equation:

$$\dot{\xi}_i = \alpha_i A_i \quad (10)$$

where A_i is the generalized force or affinity of the i th process which characterizes the distance to equilibrium^{5,7,8}. In equilibrium all A_i are zero. The term α_i is a material-dependent coefficient and ξ_i are the generalized fluxes³ which are the conjugated variables to the A_i terms. The combination of equations (9), (10) and the internal equation of state ('chemical equation of state'):

$$A_i = - \left(\frac{\partial g}{\partial \xi_i} \right)_{\lambda, T, p} \quad (11)$$

yields a differential equation for the $\xi_i(t)$. This differential equation is solved in reference 13. The solution eliminates the ξ_i in the mechanical equation of state:

$$f = \left(\frac{\partial g}{\partial \lambda} \right)_{T, \xi_i, p} \quad (12)$$

This leads to an expression for the nominal force $f^{1,13}$:

$$f(t) = W'(t) \left(1 + \frac{\Gamma}{G} \left\{ 1 - \frac{1}{\Gamma} \int_0^t m_G(t-t') \left[\frac{W'(t')}{W(t)} \right]^{1/2} dt' \right\} \right) \quad (13)$$

where $\Gamma = G_g - G$ is the relaxation strength, G_g is the maximum modulus, observed at the highest frequencies [$G_g = G(\omega \rightarrow \infty)$] and $W'(t) = \partial_\lambda W[\lambda(t)]$. The memory function, $m_G(t-t')$, is defined by the normalized relaxation

time spectrum (Figure 2):

$$m_G(t-t') = \sum_i \frac{h_i}{\tau_i} \exp\left[-\frac{(t-t')}{\tau_i}\right] \quad (14)$$

where h_i is the relative weight of the i th process in the normalized spectrum and τ_i is the relaxation time. h_i and τ_i are combined with the α_i by the relation $h_i/\tau_i = f_{11}^{(i)2}\alpha_i$. The relaxation time spectrum is derived from the measurement of the dynamic modulus $G(\omega)$ with the Schwarzl-Stavermann approximation¹¹. Every variable in equation (13) is determined by experiment so that no fitting parameter is left.

From the relaxation mode coupling model in the Onsager version follows that the relaxation spectrum is strain invariant and does not depend on the type of strain. Despite the fact that each of the relaxation modes is coupled with the equilibrium state of reference and despite the fact that the mechanical equation of state behaves non-linearly with respect to the macroscopic strain, relaxation is still treated as a linear response which satisfies a generalized version of the superposition principle.

THE TEMPERATURE DEPENDENCE OF THE RELAXATION PROCESSES

As long as the shape of the relaxation time spectrum does not change with temperature (thermorheological simple conditions), Williams, Landel and Ferry defined an empirical relationship, the WLF equation¹¹, which outlines the congruent shift of every discrete relaxation time at temperatures above the glass transition:

$$\log a_T = -\frac{C_1(T-T_S)}{C_2+T-T_S} \quad (15)$$

Stress-strain cycles of PMMA networks are well described above the glass transition with equation (13) after the relaxation time spectrum and the parameters C_1 , C_2 and T_S of equation (15) are determined by experiment. In our case $C_1 = 6.34$, $C_2 = 63.62$ and $T_S = 416.5$ K. The calculation (Figure 3) is carried out with a strain-independent relaxation time spectrum. The time-temperature relationship¹⁵ is valid despite each of the relaxation mechanisms being coupled with the network. This underlines a certain autonomy of the elementary relaxation processes.

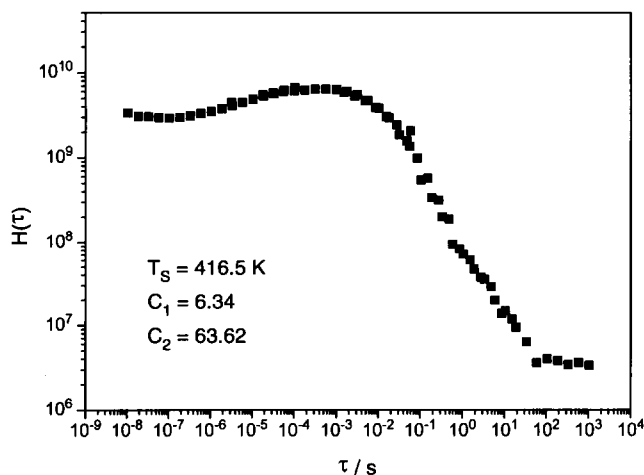


Figure 2 Relaxation time spectrum of the PMMA network of Figure 1 at 416.5 K

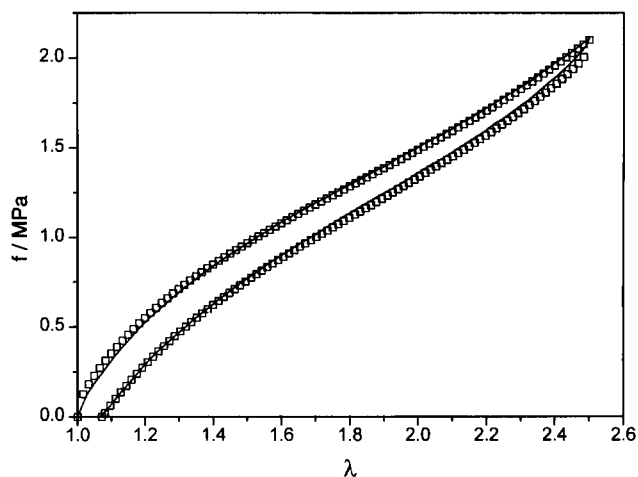


Figure 3 Experimental (□) and calculated (—) stress-strain cycles of the PMMA network at 413 K and at a strain rate $\dot{\epsilon} = 1.3 \times 10^{-2} \text{ s}^{-1}$ (parameters and relaxation spectrum as given in Figures 1 and 2)

These processes are supposed to obey the Onsager relationship [equation (10)].

It is an important fact that the relaxation time spectrum of the network is deduced from small strain experiments¹¹. A master curve is constructed with a broad frequency range including very short relaxation times by using the empirical shift procedure according to the WLF equation. The whole set of relaxation modes is thermally activated. To construct a master curve is equivalent to assuming that the thermal activation of high frequency processes follows the same rules as for those ones in the low frequency region. Because of this remarkable symmetry, every deviation from the WLF behaviour must be explained by additional effects like strain-induced activation. These considerations facilitate the following discussion where we propose how relaxation in the glass transition region may be treated.

THE WLF REGIME

Above the glass transition temperature, the whole set of relaxation modes is thermally activated. A crucial question is where the thermal activation and the WLF procedure fail depending on strain rate^{21,22}. Strain-induced activation should play an increasing role when the relaxation times are shifted to values which are much larger than the ones in the time window of experiment. The WLF equation includes its limiting temperature^{11,23}, the Vogel temperature T_0 . Below that temperature, the process of polymer segments changing place can no longer be thermally activated. This statement corresponds to imagining a rigid body with each molecular unit embedded in a harmonic potential, so that the units are fully localized. If we now ask for the limits of the WLF equation, this is equivalent to regarding the segments of a polymer chain as being located in a potential of finite height. For this reason, the process of polymer segments changing place can be enforced in the glass transition region and in the glassy state under applied strain.

First let us find out where the WLF equation is applicable. If we compare experimental stress-strain curves with calculations [using equation (13)] for various temperatures and strain rates, we are able to identify where the theory gives an exact description of the

experimental stress-strain cycles depending on the two variables $\dot{\epsilon}$ and T . Looking at the $\dot{\epsilon}-T$ plane (Figure 4), we obtain good accordance between experiment and calculation in region I (WLF regime) if the fundamental network parameters, the relaxation time spectrum and the corresponding WLF parameters are known. Calculations prove that we need the spectrum as a whole. Every relaxation mode is in operation. The triangles in Figure 4 represent measurements at a certain temperature and strain rate where the calculation of the stress-strain curves is accurate (triangles which lie within region I were omitted for clarity). For lower temperatures or larger strain rates, however, we recognize a systematic deviation of the theory from the experimental curves. Therefore, these triangles represent the strain rate dependent limit of application of the WLF equation. This limit is described by the expression:

$$-\log \dot{\epsilon} = \frac{\tilde{A}}{T - T^*} - \log \dot{\epsilon}_0$$

and

$$\dot{\epsilon}^{-1} = \dot{\epsilon}_0^{-1} \exp\left(\frac{A}{T - T^*}\right) \quad (16)$$

The triangles lie on curve (1) in Figure 4, which is computed using equation (16) and the parameters $T^* = 352.88$ K, $A = 928.77$ K and $\log \dot{\epsilon}_0^{-1} = -6.36$. For an explanation of equation (16) and for the following discussion it is useful to change to the Vogel-Fulcher equation^{11,23}:

$$\langle \tau \rangle = \langle \tau_0 \rangle \exp\left(\frac{B}{T - T_0}\right) \quad (17)$$

This is equivalent to the WLF equation. The parameters of equation (17), which are directly deduced from the WLF equation, are $B = 919.78$ K, $\log \langle \tau_0 \rangle = -6.30$ and $T_0 = T^*$. Within the limits of accuracy, the parameters in equation (17) turn out to be identical to those obtained using equation (16). We learn that the boundary of

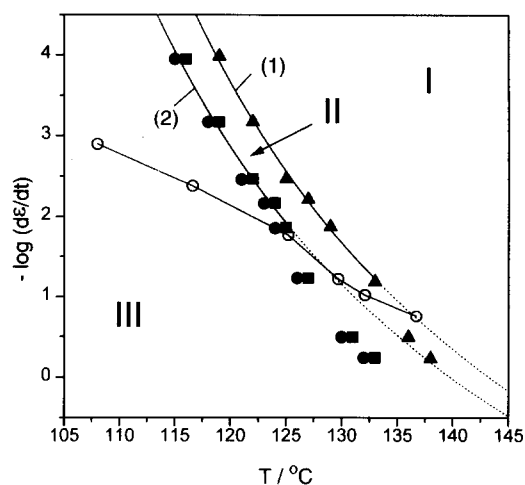


Figure 4 Logarithmic plot of the strain rate de/dt versus the absolute temperature T . Regime I is the WLF regime. In regimes II and III characteristic deviations with respect to WLF behaviour are found. In regime II every extension occurs quasi-homogeneously, while a neck is always observed in regime III; below the data points (○) the sample is heated up during extension. Curve (I) is calculated with equation (16) ($A = 928.77$ K, $\log \dot{\epsilon}_0^{-1} = -6.36$)

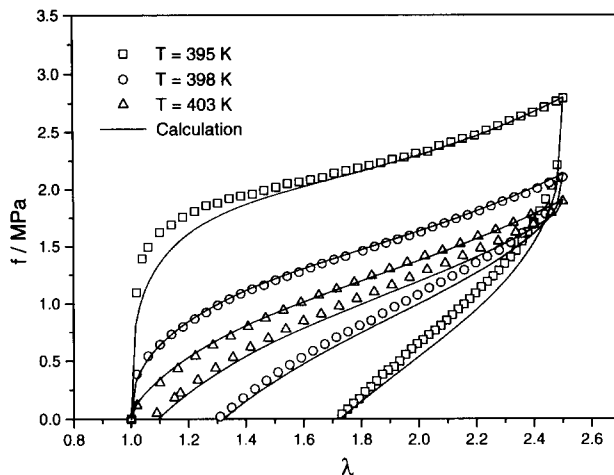


Figure 5 Stress-strain cycles at a strain rate $\dot{\epsilon} = 6.0 \times 10^{-4} \text{ s}^{-1}$. Experiment and calculation show a crossover point

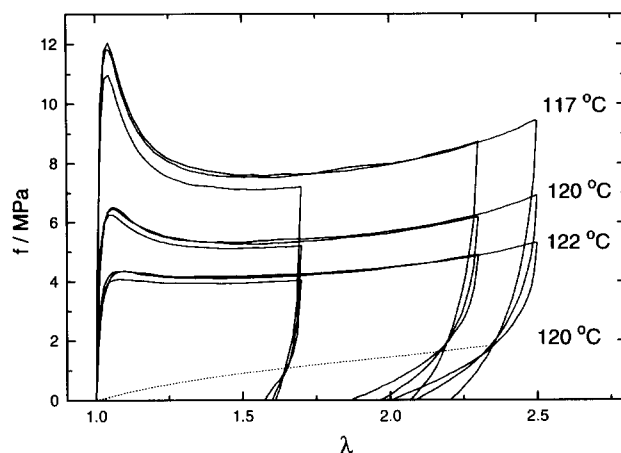


Figure 6 Stress-strain pattern of a PMMA network stretched in regime III at a strain rate $\dot{\epsilon} = 7.2 \times 10^{-4} \text{ s}^{-1}$. The temperatures are indicated in the figure. The broken line is the quasi-static equilibrium curve

application of the WLF equation is characterized by the relationship:

$$\dot{\epsilon} \langle \tau \rangle = 1 \quad (18)$$

that is correct over more than three decades of $\dot{\epsilon}$ (Figure 4). We therefore conclude that thermal activation determines the relaxation behaviour of the whole set of relaxation modes as long as the mean relaxation time $\langle \tau \rangle$ is shorter than or equal to the representative experimental period of time. In region I, the process of polymer segments changing place is only due to thermal activation. All relaxation modes run as in a polymer liquid where molecular segments or larger units are not strictly localized. A network displays locally the properties of a viscoelastic polymer liquid. However, the relaxation mechanisms are forced to co-operate due to being linked with the network. If one extends the network to the same maximum strain, the unloading curves (at different temperatures as well as at different strain rates) cross over at a defined point on the quasi-static equilibrium curve (Figures 5 and 6). Therefore, we conclude that the scalar and isotropic coupling of the relaxation modes with the network, that is identical for each mode, synchronizes the whole set of relaxation mechanisms in

the WLF regime. Every relaxation mode should always show the same strain-induced distance to equilibrium. This explains why they simultaneously cross over the equilibrium stress-strain curve at a single point. The quasi-static stress-strain curve is directly identified as the correct state of reference.

THE GLASS TRANSITION REGION

According to Figure 4 the regime beyond the WLF boundary is divided into regimes II and III. In any case, relaxation is enhanced with increasing distance to the WLF boundary. In regime II, the stress-strain pattern does not yet show a maximum at small strains, while this is typical in regime III (Figures 6 and 7). The appearance of the maximum in the stress-strain curve is accompanied with the formation of a neck. The deformation process then runs heterogeneous. Let us first describe the boundary line between regimes II and III in Figure 4 (curve (2)), the limit of mechanical stability. As long as deformation runs quasi-isothermal, the boundary line between II and III is described by equation (16) using the same A and $\log \dot{\epsilon}_0^{-1}$ as in the WLF regime. Only the reference temperature T^* must be reduced by 3.5K.

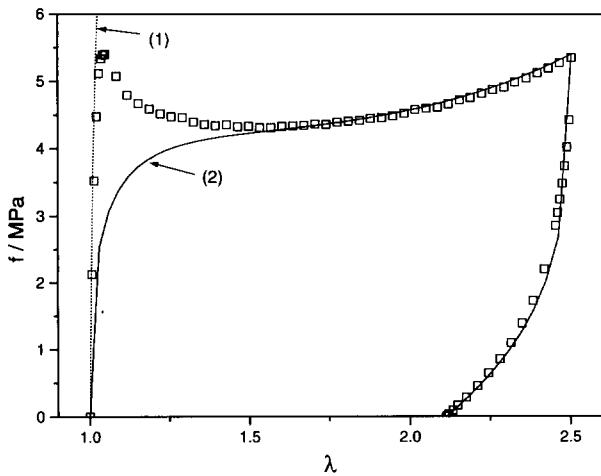


Figure 7 Stress-strain pattern of a PMMA network drawn in regime III with a strain rate $\dot{\epsilon} = 7.2 \times 10^{-4} \text{ s}^{-1}$ at 390 K. Curve (1) is computed using the WLF relation. The theoretical curve (2) is computed using the shift factor $\log a_T = 3.82$

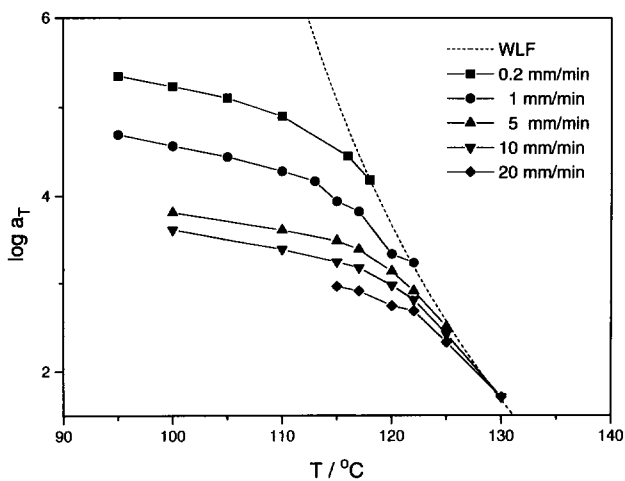


Figure 8 Empirical shift factors of a PMMA network in the temperature region of the glass transition for various strain rates

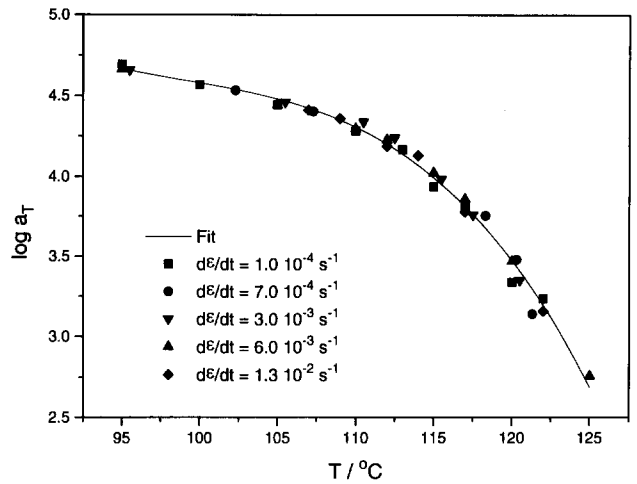


Figure 9 Master curve of the deviation of the shift factor for a PMMA network in regimes II and III. The solid line is a fit with a third-order polynomial

Non-isothermal deformation seems to be the cause for the systematic discrepancies between calculation and experiment at large strain rates (broken lines in Figure 4).

A representative example of a stress-strain cycle observed in regime III is shown in Figure 7. With the WLF parameters deduced in regime I we are able to reproduce the measurement at small extensions [Figure 7, curve (1)]. At strains of a few per cent, yielding occurs. After the neck is formed, we are able to describe the stress-strain cycle [curve (2)] in Figure 7. The shift factor has to be adjusted to a lower value as predicted by the WLF equation. The whole stress-strain pattern except the peak area is well described including the unloading curve. At sufficiently high strains the network displays thermorheological simple behaviour with a defined time-temperature relationship.

THE SHIFT PROCEDURE IN THE GLASS TRANSITION RANGE

Owing to the continuous process of vitrification it is expected that segmental motions are not only thermally but also elastically activated²⁴⁻²⁷. We want to prove that the relaxation time spectrum behaves in an elastically and rheologically simple fashion. If this holds true, the whole set of relaxation times is also uniformly shifted. The temperature-frequency relationship should be modified due to the influence of elastic effects.

In Figure 8 'stationary' shift factors are plotted for different strain rates against temperature. Independent of whether a neck is formed or not, these shift factors show the same characteristics. To confirm this we define for each strain rate, $d\epsilon/dt$, just that temperature, $T_{WLF}(d\epsilon/dt)$, below which the WLF procedure fails. To compare the various curves, each one is rescaled to an arbitrarily chosen temperature of reference $T_{WLF,0}(d\epsilon_0/dt)$. According to equation (19), T_{WLF} is given as a function of the strain rate by:

$$T_{WLF}(\dot{\epsilon}) = T^* - A \left(\log \frac{\dot{\epsilon}}{\dot{\epsilon}_0} \right)^{-1} \quad (19)$$

We arrive at the master curve illustrated in Figure 9. The master curve can be described by a third-order polynomial.

This systematic shift-factor reduction in regimes II and III must have deeper physical reasons. First, relaxation

in the glass transition region is at sufficiently large strains thermorheologically simple. Here the shape of the relaxation spectrum remains unchanged. A frequency-temperature relationship is defined. The congruent shift of all the relaxation times indicates that thermal- and strain-induced activation both modify the relaxation times in the same manner. According to Ferry¹¹ this should be influenced by a thermodynamically well defined increase of free volume during deformation.

In the stationary regime of larger strains each of the relaxation modes is dynamically equivalent. Each mode is forced into the same distance from equilibrium. The equilibrium state of reference is defined by the quasi-static strain-energy of the van der Waals network. The glassy state of a permanent network is therefore understood as a highly co-operative freezing process that defines a solid state with a well defined distance to equilibrium. This distance is characterized by a set of hidden variables.

For reasons of consistency we should be allowed to describe the whole stress-strain pattern in *Figure 7* [curve (2)] by fitting the shift factor in order to reproduce the maximum¹¹. It can be shown that in regime III the relaxing network becomes unstable beyond the stress maximum because the relaxation rates increase due to the large quantity of stored strain energy. In the glassy state, deformation occurs by forming a neck. This interesting fundamental phenomenon will be discussed in a subsequent paper.

NON-ISOTHERMAL DEFORMATION

With an i.r. camera we have measured the surface temperature during extension^{28,29}. The temperature is raised in the regime below the open circles shown in *Figure 4*. Therefore we have isothermal conditions in the area above these circles and non-isothermal conditions below the circles. This would not change the topologic features of our representation except for a small systematic decrease in the shift factor in the non-isothermal regime.

CONCLUSIONS

The results presented show many symmetries that characterize large deformation in networks. A permanent network is in the thermodynamic limit fully described up to large strains if the fundamental van der Waals parameters of equation (1), M_w , λ_m and a , are known. A van der Waals network is typified as a weakly interacting conformational gas. Fluctuations of the network junctions indicate stochastic interactions between neighbouring chains. The network is an entropy-elastic system. This is the reason why the strain-energy is equipartitioned among network chains of different lengths. The PMMA networks show a broad chain length distribution. Thus, every deformation must be inhomogeneous on a local level, because non-Gaussian chains of different lengths are individually deformed to satisfy equipartition of energy. At sufficiently large strains these characteristics are not changed in the glass transition region.

The equilibrium state of the network is in the stationary regime always the state of reference. Because a network can only be forced to small distances with respect to the equilibrium state, thermodynamics of irreversible processes is applied to describe non-equilibrium states and to formulate a constitutive equation which includes the

thermodynamic limit. A set of elementary relaxation processes in the Onsager version is defined. It is characteristic for networks that these relaxation modes are linked with the network. This is the reason why all relaxation processes are strictly synchronized during deformation. The network itself defines a 'global level'. Its predominant role is thermodynamically determined. The time-dependent response is characterized by a memory function in the classical version of linear systems. In the rubbery state the relaxation time spectrum does not depend on the applied strain or on the strain rate and shows thermorheological simplicity. This holds true up to large strains. The WLF equation is appropriate for describing the temperature-induced shift of the relaxation time spectrum for temperatures above the glass transition temperature.

In the time-temperature space, the WLF regime is limited by a well defined boundary. This boundary is given by the condition $\dot{\epsilon}\langle\tau\rangle = 1$. The shift factor modification of the time-temperature relationship displays universal features even in regimes II and III. This is manifested by the existence of a universal scaling law for all strain rates (*Figure 9*). The relaxation behaviour at large strains remains thermorheologically simple with the same relaxation time spectrum as in the rubbery state. The relaxation processes are also strictly synchronized, controlled from the global level. Hence, activation of the process of polymer chain segments changing place must be identical for each relaxation process. The individual response is controlled by these symmetries enforcing for example necessarily an individual state of relaxation for each different relaxation mode to always adjust the same relative distance to equilibrium.

This relaxation mode coupling model appears to be adequate to describe the universal features of relaxation at large strains in the rubbery state as well as in the glass transition region. The memory function as a manifestation of the linear Onsager equation is typical for polymer networks. It is impossible even in the glass transition region and under large extensions to bring a network in a large distance to equilibrium. The time-dependent set of constraints, as represented by the hidden variables, guarantees the necessary homogeneity. In this situation, any attempt to identify the molecular processes, represented by the phenomenological relaxation time spectrum, is of interest.

ACKNOWLEDGEMENTS

The support of the Deutsche Forschungsgemeinschaft (Sonderforschungsbereich 239) is gratefully acknowledged. We also thank Dr J. Lehmann and the RÖHM Company (Darmstadt) for supplying the PMMA networks.

REFERENCES

- 1 Ambacher, H., Enderle, H. F., Kilian, H. G. and Sauter, A. *Colloid Polym. Sci.* 1989, **80**, 209
- 2 Enderle, H. F., Kilian, H. G. and Vilgis, T. *Colloid Polym. Sci.* 1984, **262**, 696
- 3 deGroot, S. R. and Mazur, P. 'Non-equilibrium Thermodynamics', North Holland, Amsterdam, 1962

- 4 Meixner, J. Z. *Naturforsch.* 1954, **9**, 654
- 5 Meixner, J. and Reik, H. G. 'Thermodynamik der irreversiblen Prozesse', Springer, Berlin, 1963
- 6 Garcia-Colin, L. S. and Uribe, F. J. *J. Non-Equilib. Thermodyn.* 1991, **16**, 89
- 7 Onsager, L. *Phys. Rev.* 1931, **37**, 405
- 8 Onsager, L. *Phys. Rev.* 1931, **38**, 2265
- 9 Gutzow, I. and Dobrev, A. *Polymer* 1992, **33**, 451
- 10 Scherer, G. W. 'Relaxation in Glass and Composites', John Wiley and Sons, New York, 1986
- 11 Ferry, J. D. 'Viscoelastic Properties of Polymers', John Wiley and Sons, New York, 1980
- 12 Kraus, V., Kilian, H. G. and v. Soden, W. *Prog. Colloid Polym. Sci.* 1992, **90**, 27
- 13 Kraus, V. *PhD Thesis* Universität Ulm, 1993
- 14 Williams, M. L., Landel, R. F. and Ferry, J. D. *J. Am. Chem. Soc.* 1955, **77**, 3701
- 15 Binder, K. personal communication, 1992
- 16 Haward, R. N. 'The Physics of Glassy Polymers', Applied Science, London, 1973
- 17 Kinloch, A. J. and Young, R. J. 'Fracture Behaviour of Polymers', Elsevier, London, 1973
- 18 Vilgis, T. and Kilian, H. G. *Colloid Polym. Sci.* 1986, **264**, 131
- 19 Kilian, H. G. and Unseld, K. *Colloid Polym. Sci.* 1985, **264**, 9
- 20 Callen, H. B. 'Thermodynamics', John Wiley and Sons, New York, 1960
- 21 Chow, T. S. *J. Mater. Sci.* 1990, **25**, 957
- 22 Tsai, S. W., Halpin, J. and Pagano, N. J. 'Composite Materials Workshop', Technomic, Stanford, 1988
- 23 Vogel, H. *Phys. Z.* 1921, **22**, 645
- 24 Matsouka, S. *Mater. Res Soc.* 1978, **79**, 325
- 25 Adam, G. and Gibbs, J. H. *J. Chem. Phys.* 1965, **43**, 139
- 26 Doolittle, A. K. *J. Appl. Phys.* 1951, **22**, 1471
- 27 Kovacs, A. J. *Fortschr. Hochpolym. Forsch.* 1970, **3**, 394
- 28 Koenen, J. *PhD Thesis* Universität Ulm, 1991
- 29 Saile, M. *Diplom Thesis* Universität Ulm, 1992